JGR Atmospheres

RESEARCH ARTICLE
10.1029/2019JD030804

Bias Correction of High-Resolution Regional Climate Model Precipitation Output Gives the Best Estimates of Precipitation in Himalayan Catchments

Daniel Bannister[1,2], Andrew Orr[1], Sanjay K. Jain[3], Ian P. Holman[4], Andrea Momblanch[4], Tony Phillips[1], Adebayo J. Adeloye[5], Boris Snapir[4], Toby W. Waine[4], J. Scott Hosking[1], and Clare Allen-Sader[1]

[1]British Antarctic Survey, Cambridge, UK, [2]Satavia Ltd., Cambridge, UK, [3]National Institute of Hydrology, Roorkee, India, [4]Cranfield Water Science Institute, Cranfield University, Cranfield, UK, [5]Institute for Infrastructure and Environment, Heriot-Watt University, Edinburgh, UK

Key Points:
- The ability of the Weather Research and Forecasting model at high resolution to simulate precipitation over Himalayan catchments was mixed
- Applying a nonlinear bias-correction method to the model output resulted in much better estimates of precipitation over both catchments
- The bias-corrected model output provided better estimates of mean and extreme precipitation than gridded precipitation products

Supporting Information:
- Data S1
- Figure S1
- Figure S2
- Figure S3
- Figure S4

Correspondence to:
D. Bannister and A. Orr,
daniel.bannister@satavia.com;
anmcr@bas.ac.uk

Citation:
Bannister, D., Orr, A., Jain, S. K., Holman, I. P., Momblanch, A., Phillips, T., et al. (2019). Bias correction of high-resolution regional climate model precipitation output gives the best estimates of precipitation in Himalayan catchments. *Journal of Geophysical Research: Atmospheres*, *124*, 14,220–14,239. https://doi.org/10.1029/2019JD030804

Received 11 APR 2019
Accepted 12 DEC 2019
Accepted article online 14 DEC 2019
Published online 26 DEC 2019

Abstract The need to provide accurate estimates of precipitation over catchments in the Hindu Kush, Karakoram, and Himalaya mountain ranges for hydrological and water resource systems assessments is widely recognized, as is identifying precipitation extremes for assessing hydro-meteorological hazards. Here, we investigate the ability of bias-corrected Weather Research and Forecasting model output at 5-km grid spacing to reproduce the spatiotemporal variability of precipitation for the Beas and Sutlej river basins in the Himalaya, measured by 44 stations spread over the period 1980 to 2012. For the Sutlej basin, we find that the raw (uncorrected) model output generally underestimated annual, monthly, and (particularly low-intensity) daily precipitation amounts. For the Beas basin, the model performance was better, although biases still existed. It is speculated that the cause of the dry bias over the Sutlej basin is a failure of the model to represent an early-morning maximum in precipitation during the monsoon period, which is related to excessive precipitation falling upwind. However, applying a nonlinear bias-correction method to the model output resulted in much better results, which were superior to precipitation estimates from reanalysis and two gridded datasets. These findings highlight the difficulty in using current gridded datasets as input for hydrological modeling in Himalayan catchments, suggesting that bias-corrected high-resolution regional climate model output is in fact necessary. Moreover, precipitation extremes over the Beas and Sutlej basins were considerably underrepresented in the gridded datasets, suggesting that bias-corrected regional climate model output is also necessary for hydro-meteorological risk assessments in Himalayan catchments.

1. Introduction

The Hindu Kush, Karakoram, and Himalaya (HKKH) mountain ranges are the source of many of the major rivers of the Indian subcontinent, including the Indus, the Ganga, and the Brahmaputra, which support the lives of over a billion people by providing water resources for domestic consumption, industry, irrigation, hydro-electric power, etc (Eriksson et al., 2009). The rivers are mainly fed by precipitation resulting from the mountains lifting the larger-scale background flow patterns (Bookhagen & Burbank, 2010; Medina et al., 2010; Norris et al., 2015, 2017; Palazzi et al., 2013; Wulf et al., 2010; Yadav et al., 2012). For example, eastern HKKH drainage basins receive approximately 70% of their annual precipitation in summer from the Indian monsoon impinging on the mountains, which falls predominantly as rain that quickly enters the river systems (Burbank et al., 2012). By contrast, catchments in the Western HKKH region receive approximately half their annual precipitation from extratropical storms in the winter months, which falls predominantly as snow, so that most of the ensuing discharge into the river systems comes from snow and glacier melt runoff from the spring onward (Jain et al., 2010; Norris et al., 2015; Singh & Jain, 2003). In addition, localized dynamical and physical processes, such as the modification of flow by small-scale topographic features and thermally induced valley circulations, can result in sharp increases in the spatial and temporal variability of precipitation rates (Das et al., 2006; Dimri et al., 2017; Norris et al., 2017; Orr et al., 2017; Potter et al., 2018). Such interactions also make the foothills of the HKKH particularly susceptible to precipitation extremes (Karki et al., 2017; Sigdel & Ma, 2017), which in turn can trigger hydro-meteorological hazards (such as floods, landslides, and droughts) that can cause large losses of life and property and hamper socio-economic development of vulnerable communities (Eriksson et al., 2009).

The development of effective strategies to mitigate water stress problems requires good knowledge of water resources originating in the HKKH region, which are commonly investigated using hydrological (Jain et al., 2010; Singh & Jain, 2003) and water resource systems (Chinnasamy et al., 2015; Momblanch et al., 2019; Sharma & De Condappa, 2013) models. In mountainous regions, hydrological models are highly sensitive to errors in precipitation data, which is one of the key inputs used to force them (Andermann et al., 2011; Li et al., 2017; Meng et al., 2014; Remesan & Holman, 2015; Wulf et al., 2016). Important factors include knowing the precipitation frequency, intensity, timing, spatial distribution, and number of rainy days. Additionally, assessing the vulnerability to hydro-meteorological hazards in the HKKH region requires a good understanding of precipitation extremes (Karki et al., 2017; Panday et al., 2014; Roy, 2008; Sanjay et al., 2017; Sigdel & Ma, 2017). However, establishing this information from in situ measurements in the HKKH region is highly challenging as their scarcity, questionable reliability, and uneven distribution make the delineation of sharp precipitation gradients that characterize this region difficult (Anders et al., 2006; Immerzeel et al., 2015; Norris et al., 2017; Roy, 2008; Winiger et al., 2005).

Moreover, establishing precipitation information from the long-term daily gridded dataset APHRODITE (Asian Precipitation Highly Resolved Observational Data Integration Towards Evaluation of Water Resources; Yatagai et al., 2012) is therefore also fraught with difficulties. Since it is based on the interpolation of in situ precipitation measurements, the accuracy of APHRODITE is severely compromised in the HKKH region due to both data-scarcity as well as inadequacies in interpolation methods (Bhardwaj et al., 2017; Hussain et al., 2017). The reliability of the gridded precipitation dataset based on TRMM (Tropical Rainfall Measuring Mission; Huffman et al., 2007) satellite estimates over the HKKH region is similarly compromised, as TRMM has deficiencies in detecting local orographically induced precipitation (particularly over glaciated areas), which requires adjustment using in situ measurements (Andermann et al., 2011; Yin et al., 2008). Additionally, given their rather coarse spatial resolution and dependence on the assimilation of meteorological observations, precipitation estimates over the HKKH region from global atmospheric reanalysis datasets such as ERA-Interim (Dee et al., 2011) are also unsuitable for forcing hydrological models (Ma et al., 2009).

Using a regional climate model to dynamically downscale coarse-resolution reanalysis or global climate model data to high spatial resolution (<10 km) over data-sparse mountainous regions is one method for providing sufficiently detailed precipitation information for driving hydrological and water resources models and estimating precipitation extremes for impact assessments (e.g., Akhtar et al., 2008; Ali et al., 2015; Ghosh & Dutta, 2012; Narula & Gosain, 2013; Li et al., 2016; Nepal, 2016; ul-Hasson, 2016; Sanjay et al., 2017]. Subsequent biases in the downscaled precipitation output can be reduced using postprocessing techniques that correct important statistical properties of the simulated precipitation distribution so that they match the available observations, resulting in realistic forcing data for hydrological streamflow simulations (Teutschbein & Seibert, 2012). However, despite the fine spatiotemporal resolution and improved representation of key dynamical and physical processes of a regional climate model, their representation of precipitation (and the subsequent impact of bias correction) over the HKKH remains uncertain. For example, previous studies examining the performance of the Weather Research and Forecasting (WRF) model at high resolution in the HKKH region have typically focused on either one small river catchment or over larger regions that considered only a limited number of in situ measurements for relatively short periods of time of 1 year or less (Bonekamp et al., 2018; Collier & Immerzeel, 2015; Li et al., 2017; Maussion et al., 2011; Norris et al., 2017; Orr et al., 2017), therefore failing to fully assess the model's ability to reproduce the actual detailed patterns of precipitation. Furthermore, though multiple studies have shown the importance of bias correction of precipitation over topographically complex regions (e.g., Bordoy & Burlando, 2013; Lafon et al., 2013; Teutschbein & Seibert, 2012), the usefulness of such methods over the HKKH has yet to be conclusively proven (Shrestha et al., 2017).

To address these deficiencies, the objectives of this study are the following:

1. Undertake a comprehensive comparison of raw (uncorrected) and bias-corrected precipitation output from a 33-year high-resolution regional climate model hindcast using the WRF model of two contrasting Himalayan river basins, the Beas, and the Sutlej, against an extensive network of in situ measurements.

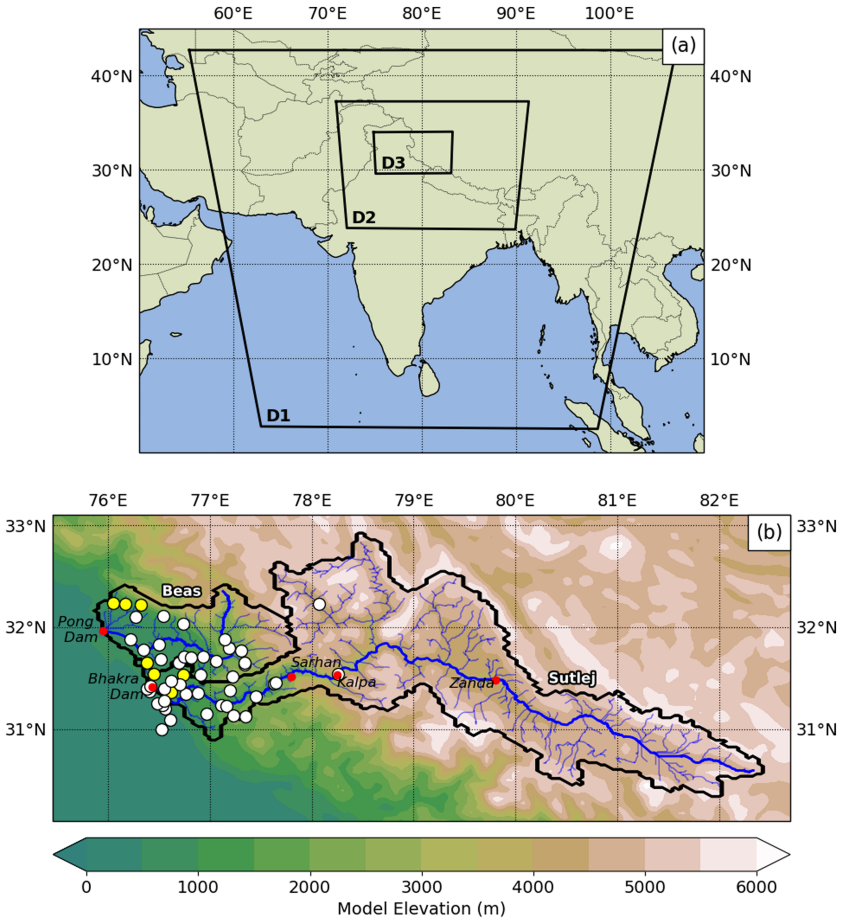

Figure 1. (a) Map showing the three nested domains used by the Weather Research and Forecasting (WRF) model (black solid lines) at spatial resolutions of 45 km (D1), 15 km (D2), and 5 km (D3). The innermost 5-km domain contains the Beas and Sutlej river basins. (b) Map of the innermost 5-km domain showing the catchment boundaries (black), water course (bold blue), elevation of the WRF model terrain (shading; at 5 km resolution), locations of the 44 in situ precipitation measurements used in the bias correction (white circles, each consisting of at least six continuous years of data), and the seven used for the independent validation of the bias-corrected WRF output (yellow circles, each consisting of less than six continuous years of data), and the main tributaries (thin blue) of the Beas (down to the Pong Dam) and the Sutlej (down to the Bhakra Dam) river basins. Locations referred to in the main text are indicated with red circles.

2. Compare the accuracy of precipitation estimates from three gridded datasets (TRMM, APHRODITE, and ERA-Interim) against the bias-corrected WRF model output over the same two river basins.
3. Investigate precipitation extremes in the two basins based on both the bias-corrected WRF model output and the three gridded datasets.

Located in northeast India (Figure 1a), the Beas and the Sutlej river basins are both major tributaries to the Indus River. With a catchment area of 63,803 km^2 (above the Bhakra dam), the Sutlej River basin is the largest tributary of the Indus and has its source in Western China. The Beas River basin is substantially smaller with a catchment area of 12,286 km^2 (above the Pong dam), and its headwaters exist wholly within India. Both basins reach elevations of approximately 4,000 m above sea level (asl) and straddle the western Hindu-Kush Karakoram and eastern Himalaya regions (Figure 1b). As such, precipitation across these basins is influenced by both westerly midlatitude perturbations during winter and early spring, as well as the summer monsoon. Understanding the performance of the TRMM, APHRODITE, and ERA-Interim in the HKKH region is important as they have been used for water budget studies, validation of regional climate model output, and extreme precipitation analysis without any attempt to assess the quality of their data.

2. Data and Methods

2.1. Datasets

Daily total precipitation measurements for at least six continuous years between 1980 and 2012 (i.e., long enough for a reasonable representation of the precipitation climatology) were collected from 44 sites across the Sutlej (27 stations) and Beas (17 stations) catchments, ranging in elevation from 284- to 3,639-m asl. The data were supplied by the Bhakra Beas Management Board and the Indian Meteorological Department (via Wulf et al., 2016). Data from a further 56 sites were excluded from this study as they either failed conventional quality control checks (such as double mass curve analysis and metadata checks) or because they measured snowfall only. Additionally, data from seven sites were collected that passed the above checks but consisted of less than 6 years of continuous observations. See Figure 1b for the location of the sites.

For TRMM, we used algorithm 3B42 (version 7), which merges satellite and in situ data to produce a monthly bias corrected gridded precipitation dataset covering the study region from 1998 to the present at 0.25° spatial resolution (Huffman et al., 2007). For APHRODITE, we used the Monsoon Asian Region precipitation V1101 dataset (available from 1951 to 2007) at 0.25° spatial resolution (Yatagai et al., 2012). ERA-Interim reanalysis is a gridded dataset at approximately 0.7° spatial resolution, available from 1979 to present (Dee et al., 2011).

2.2. The WRF Model

We used version 3.8.1 of the Advanced Research WRF model, which uses a fully compressible, nonhydrostatic dynamical core, with a terrain-following pressure coordinate in the vertical (Skamarock et al., 2008). The model was run on a series of three nested domains (Figure 1a). The innermost domain had 157×100 grid points with a 5-km spatial resolution and included the Beas and Sutlej river basins. This was nested within a domain covering the whole of the HKKH region with 124×100 grid points and a 15-km spatial resolution and an outermost domain covering the whole of the Indian subcontinent with 100×100 grid points and a 45-km spatial resolution. All domains had 30 vertical levels between the surface and the model top at 50 hPa. The model was forced with atmospheric initial and boundary conditions derived from ERA-Interim. See Table 1 for a summary.

To determine the optimum model setup for the study area, a preliminary evaluation of the sensitivity to the choice of parameterizations schemes was conducted by running the model for two 1-month periods (during a winter and a summer season), and comparing the model output against the Moderate Resolution Imaging Spectroradiometer (MODIS)/Terra snow cover dataset (Hall et al., 2002; Shukla et al., 2016) and the available in situ precipitation observations (not shown). Based on these tests, the physics options selected included the longwave Rapid Radiative Transfer Model (RRTM) scheme (Mlawer et al., 1997) in conjunction with the shortwave Dudhia scheme (Dudhia, 1989), the Mellor-Yamada Nakanishi and Niino (MYNN) planetary boundary layer scheme (Nakanishi & Niino, 2006), the Morrison double-moment microphysics scheme (Morrison et al., 2009), the Kain-Fritsch cumulus scheme (Kain, 2004) on the 15 and 45 km domains only, and the Noah land-surface model (Chen & Dudhia, 2001). See Table 1 for a summary.

Following the approach of Collier and Immerzeel (2015) to improve the simulation of precipitation in topographically complex environments where the model vertical levels are significantly sloped, horizontal diffusion was computed in physical space rather than along model levels. In addition, spectral nudging was applied to horizontal winds, temperature, geopotential temperature, and humidity in the outermost WRF domain only, on vertical levels above mountain crest height. To correctly account for slope effects and asymmetric irradiation effects, such as self-shadowing and varying incident solar radiation, the radiation parameterization (Garnier & Ohmura, 1968) was used in the innermost (5 km) domain.

Comparison of digital outlines of glaciers from the Randolph Glacier Inventory version 5.0 (RGI V5; Pfeffer et al., 2014) with the default land use/glacier mask used by WRF (based on the USGS (U.S. Geological Survey) dataset) showed that the area of glaciers in the HKKH region is greatly underestimated in the WRF USGS dataset (not shown). Therefore, the glacier mask used in all three model domains was updated using RGI V5, similar to Collier and Immerzeel (2015) and Orr et al. (2017). The soil categories and vegetation parameters were also updated to be consistent with the revised glacier mask. To evaluate the possible impact of nonstationary land type during the period examined, sensitivity tests were also conducted by running the model for two 1-month periods with MODIS land cover data (Friedl & Sulla-Menashe, 2015)

Table 1
Summary of WRF Configuration

Domain configuration	Settings	References
Projection	Lambert conformal conic, with latitude of true scale at 30°N, central longitude at 80°E	
Centre of outer domain	23°N, 81°E	
No. vertical levels	30	
Model top	50 hPa	
Nesting	One-way nesting	
Forcing	ERA-Interim (0.7 × 0.7°, updated 6 hourly)	Dee et al. (2011)
Topography	90-m Shuttle Radar Topography Mission (SRTM)	Jarvis et al. (2008)
Land surface type	USGS 24-category land use, Randolph Glacier Inventory (version 5)	Pfeffer et al. (2014)
Physics		
Radiation	Rapid Radiative Transfer Model (RRTM), Dudhia	Mlawer et al. (1997), Dudhia (1989)
Microphysics	Morrison	Morrison et al. (2009)
Planetary boundary layer	Mellor-Yamada Nakanishi and Niino (MYNN 2.5)	Nakanishi and Niino (2006)
Land surface	Unified Noah Model	Chen and Dudhia (2001)
Cumulus	Kain-Fritsch	Kain (2004)
Dynamics		
Top boundary condition	Rayleigh damping	
Diffusion	Calculated in physical space	

Abbreviations: USGS: U.S. Geological Survey; WRF: Weather Research and Forecasting.

representative of 2001 and 2013, which showed negligible differences in terms of precipitation and snow cover (not shown). To deal with the complex terrain, the topography was derived from the 90-m Shuttle Radar Topography Mission (SRTM) dataset (Jarvis et al., 2008).

The optimized model was run continuously for one calendar year beginning on 15 December, reinitializing every year between 1980 and 2012 (i.e., a total of 33 years), with boundary conditions updated every 6 hr. This included a 16-day spin-up period for each initialization so that the subsurface soil moisture fields stabilized (Collier & Immerzeel, 2015). Forcing between domains was one way.

Only model output from the innermost (5 km) domain are examined, which was archived every hour. Where comparisons are performed against individual sites and the WRF output, the output for the model cell that contains the measurement site is taken as representative for that site, that is, a nearest-neighbor approach, involving no interpolation.

2.3. Bias Correction Method

In order to correct the mean and variance statistics of the WRF precipitation output to match the daily in situ observations, we used a power transformation first proposed by Leander and Buishand (2007). The corrected modeled daily precipitation P^* was calculated from the raw (uncorrected) model daily precipitation amount P (taken from the nearest grid point to each station) using

$$P^* = aP^b \tag{1}$$

where a and b are scaling parameters. Only observations from the 44 sites with data available for at least six continuous years were used in the bias correction, with data from the remaining seven sites used to perform an independent validation of the corrected output. Because we want to apply the bias correction to gridded model output in the entire inner domain, we extended the methodology of Terink et al. (2010; who also used this method to bias correct regional climate model output in the topographically complex Rhine basin) by (i) determining values of a and b for each of the 44 sites for every 5-day period of the year; (ii) demonstrating that the values of these parameters were dependent on elevation, enabling use of a least squares method to fit a power-law function to the a and b parameters for each five-day period as a function of model elevation; and (iii) using these derived regression relationships to apply a correction to the value of P for all model grid cells within the Beas and the Sutlej catchments based on elevation.

For step one, we determined values of a and b for each of the 44 sites for every 5-day period of the year based on averages of all the available data between 1980 and 2012 (note that this assumes that the values of a and b

for each 5-day block are the same for any year). The effect of sampling variability was reduced by employing a window that included 30 days before and after each 5-day period, that is, using a window length of 65 days to calculate statistics, and subdividing the year into 73 blocks of 5 days. Note that a number of window lengths from 105 to 15 days were considered, including 65 days (not shown). In each case the values of a and b were computed, and the mean biases compared. This showed that a 65-day window gave the lowest biases. See Terink et al. (2010) for further details. The value of b was first determined iteratively for each of the 5-day periods, such that the coefficient of variation of P^* matches that of the observed daily precipitation. As a is a linear scaling factor, it affects both the mean and the standard deviation equally, which allows this method to determine b independently of a. The values of a for each of the 5-day periods was subsequently determined by matching the mean of P^* to the observed mean. For the two highest sites, due to their very low precipitation frequencies, the iterative method used to derive a value for the b parameter failed. For this reason, these two sites were excluded from the derivation of the elevation-dependence bias correction parameters below. Note that the observations at these sites were nonetheless included in the comparisons between the observed and the modeled and bias-corrected precipitation described in section 3 below.

For step two, as well as the values of a and b being dependent on elevation, they also showed distinct differences between the two basins. Therefore, in order to apply a correction to the value of P for all model grid cells within the Beas and the Sutlej catchments, the least squares method was used to fit a power-law function to the a and b parameters for each 5-day period as a function of model elevation, with each of the two basins treated separately. For each basin, the least squares fitting and subsequent regression equation give a "multiplier" (c_a and c_b) and "power" (d_a and d_b) terms for each of the 5-day periods, which was then used to calculate values of the a and b parameters for each of the model grid cells within the basin using

$$a = c_a H^{d_a} \quad \text{and} \quad b = c_b H^{d_b} \tag{2}$$

where H is the model elevation for the model grid cell, thus enabling P^* to be computed throughout the Beas and Sutlej catchments. The results of the fitting are shown in Figures S1 to S4 in the supporting information, demonstrating that the power-law function gives a largely reasonable (statistically robust) fit for the elevation dependence of the a parameter (b parameter) for the sites in the Beas basin for June to October, as well as April (May to October, as well as January and February), while for the Sutlej basin the fit is statistically robust for the a parameter (b parameter) from April to December, as well as January (June to October). For periods when the elevation dependence is not statistically significant, this is because the regression line is close to flat (and hence that the parameter a or b does not show significant elevation dependence). This also means that for these periods, the parameters generated by applying the power-law function are similar (at all elevations) to the means of the parameters already determined to give the best fit for the mean and variance of the precipitation distribution at the observational sites. We therefore used the power-law function to derive parameters a and b for all periods, not just those for which the elevation dependence was deemed to be significant. Note that above around 3,000 m, the value of the a parameter generally tends toward zero, while the b parameter generally tends toward one. As a result, the bias correction method has little influence at high (>3,000 m) altitudes. Figure S5 shows the annual time series of the multiplier and power terms determined for both the a and b parameters for both basins, which are statistically robust for the same periods identified in Figures S1 to S4, that is, in particular June to October, which includes the monsoon period from June to September.

As previously mentioned, using a precautionary approach, observations of precipitation from an additional seven stations were not included in the bias correction due to their short and/or fragmented nature. This was done in order to reduce any statistical discontinuities in the elevation-dependent regressions, since the data from these sites are not homogenous samples of precipitation variability in this region. Also as previously mentioned, the derivation of the b bias-correction parameter failed for 2 of the 44 remaining sites. Therefore, having used the observations from 42 of the 44 remaining sites in order to build up the most statistically robust elevation-dependent regression, the data from the remaining seven sites were used to perform an independent validation of the corrected output. Table S6 in the supporting information compares how well the raw WRF model precipitation output at a spatial resolution of 5 km (hereafter simply referred to as WRF output) and bias-corrected WRF output at a spatial resolution of 5 km (hereafter simply referred to as bias-corrected WRF output) reproduce the in situ observations from the seven independent sites deliberately withheld from the bias correction. For annual as well as seasonal amounts, Table S6 demonstrates

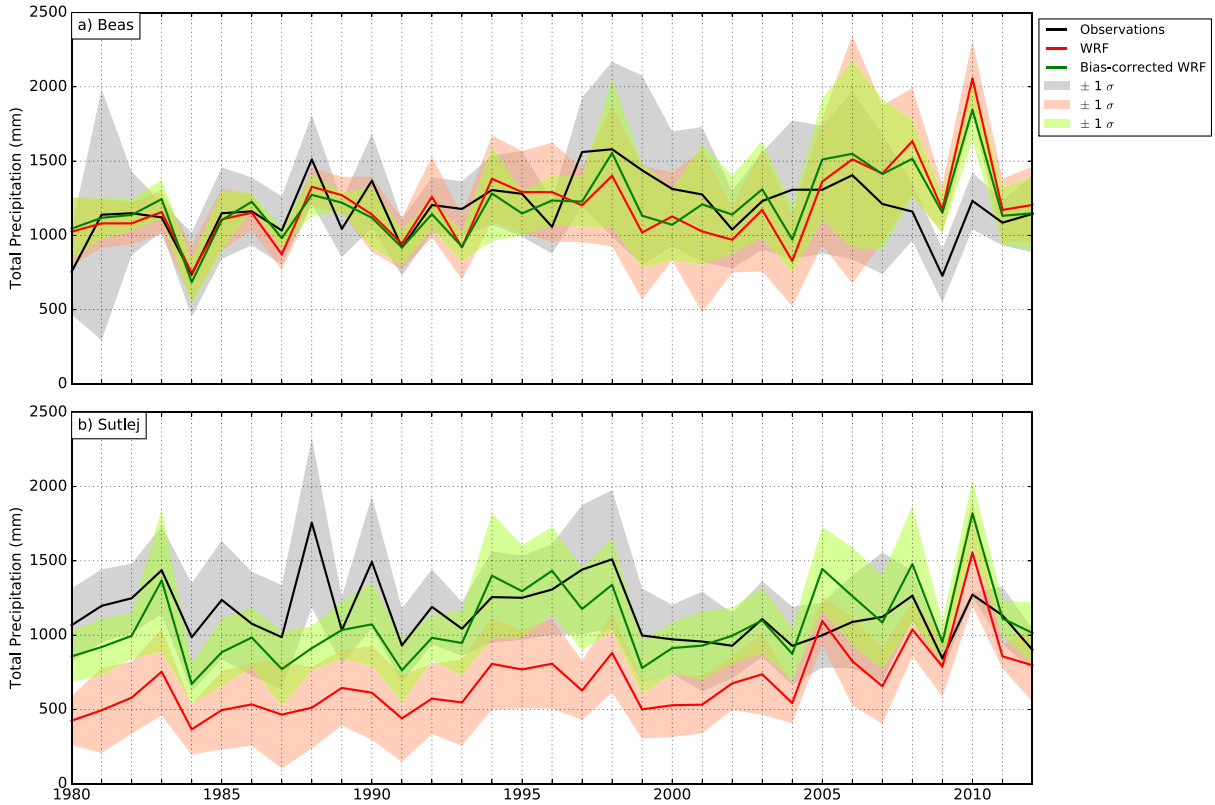

Figure 2. Comparison of (a) Beas and (b) Sutlej basin-averaged annual precipitation from the in situ observations (black), Weather Research and Forecasting (WRF) output at a spatial resolution of 5 km (red), and bias-corrected WRF output (green) for the time period 1980 to 2012. The (respective) shading indicates ±1 standard deviation away from the annual mean.

that the bias based on the bias-corrected WRF output is (often considerably) smaller than the WRF model output for five of the seven sites.

2.4. Precipitation Indices

The occurrence of moderate to heavy daily precipitation events are identified using three indices: (i) the maximum precipitation amount in five consecutive days (Rx5day), (ii) the number of days with daily precipitation ≥20 mm (R20), and (iii) the precipitation total when daily precipitation is ≥95th percentile (R95T). In addition, the persistence of precipitation is identified using two indices: (i) the maximum number of consecutive dry days (CDDs; days receiving <0.2 mm of precipitation) and (ii) the maximum number of consecutive wet days (CWDs; days receiving ≥0.2 mm of precipitation).

3. Results

3.1. Assessment of WRF Model and Bias-Corrected Precipitation

Figures 2–5 evaluate how well the WRF output and bias-corrected WRF output reproduce the 44 in situ observations of precipitation over the Beas and Sutlej basins on annual, monthly, and daily timescales.

Figure 2 compares the basin-averaged total annual precipitation amounts. For the Beas basin there is generally good overall agreement between the observations and WRF output, with the model particularly capturing total annual amounts and variance along with interannual variability between 1980 and 1995. This is also apparent from the model statistics, listed in Table 2. However, WRF is systematically too dry in the Sutlej basin (Figure 2b); for example, the bias in annual precipitation is −470.7 mm, giving a relative error of around −40% (Table 2). Figure 3 demonstrates that this dry bias is most evident at stations at lower elevations (particularly below 1,000 m asl), with the model performance at lower elevations also characterized by a relatively high root-mean-square error (RMSE) and relative error, and low correlation. To explore the

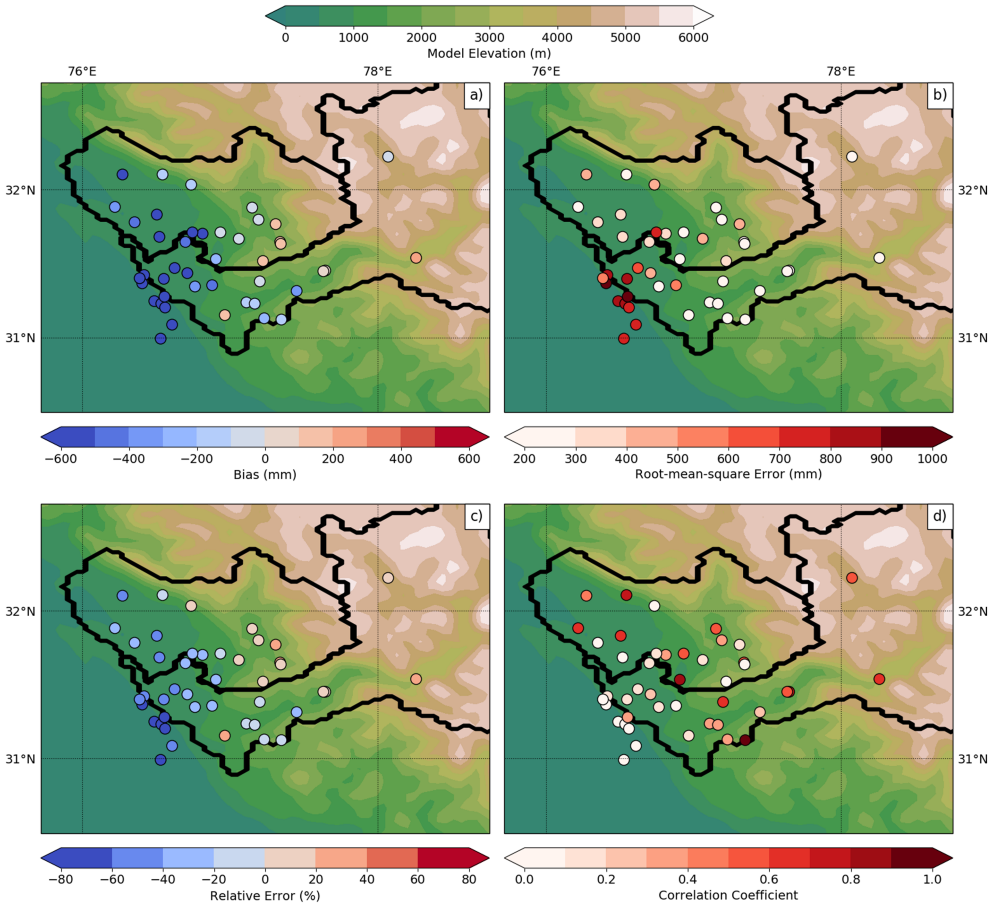

Figure 3. Error statistics for annual precipitation at each of the 44 sites in the Beas and Sutlej river basins based on output from the Weather Research and Forecasting (WRF) model at a spatial resolution of 5 km for the time period 1980 to 2012. Filled circles show the (a) bias, (b) root-mean-square error, (c) relative error, and (d) correlation coefficient. Also shown is the elevation of the WRF model terrain at a spatial resolution of 5 km (shading) and the catchment boundaries for the Beas and Sutlej basins (black). Note that the panels only show the portion of the innermost domain that includes the measurement sites.

elevation dependence of the model performance further, a linear least squares fit of the annual mean bias and model elevation was calculated. A significant regression was found, with an r^2 value of 0.50, which is statistically significant at the 99% confidence level ($p < 0.01$). Individually, the Beas and Sutlej stations were found to have an r^2 value of 0.67 and 0.61, respectively ($p < 0.01$). The dry bias for the Sutlej basin is markedly reduced by bias correcting the WRF output (Figure 2), resulting in a considerable reduction in the annual precipitation bias (from −470.7 to −74.4 mm), as well as a reduction in the RMSE (from 547.7 to 259.4 mm; Table 2). For the Beas basin, the impact of bias correcting is much smaller but still an improvement increasing the correlation value from 0.33 to 0.48.

Figure 4 compares the basin-averaged annual seasonal cycle of precipitation. For each of the basins, the in situ observations show a pronounced peak reaching 250 mm per month during the monsoon (June-July-August-September), compared to values between 50 and 100 mm per month during winter (January-February-March) and premonsoon (April-May), and less than 50 mm per month during post-monsoon (October-November-December). As such, the monsoon season is the main contributor to the annual precipitation totals in both catchments. The WRF model reproduces the seasonal contrasts of the relatively dry premonsoon and postmonsoon seasons compared to the much wetter monsoon months. However, Figure 4b shows a pronounced dry bias during the monsoon in the Sutlej basin (which is predominately responsible for the dry bias on annual timescales apparent in Figure 2b), as well a smaller dry bias during winter and premonsoon. By contrast, the WRF output has a relatively small wet bias in the Beas basin

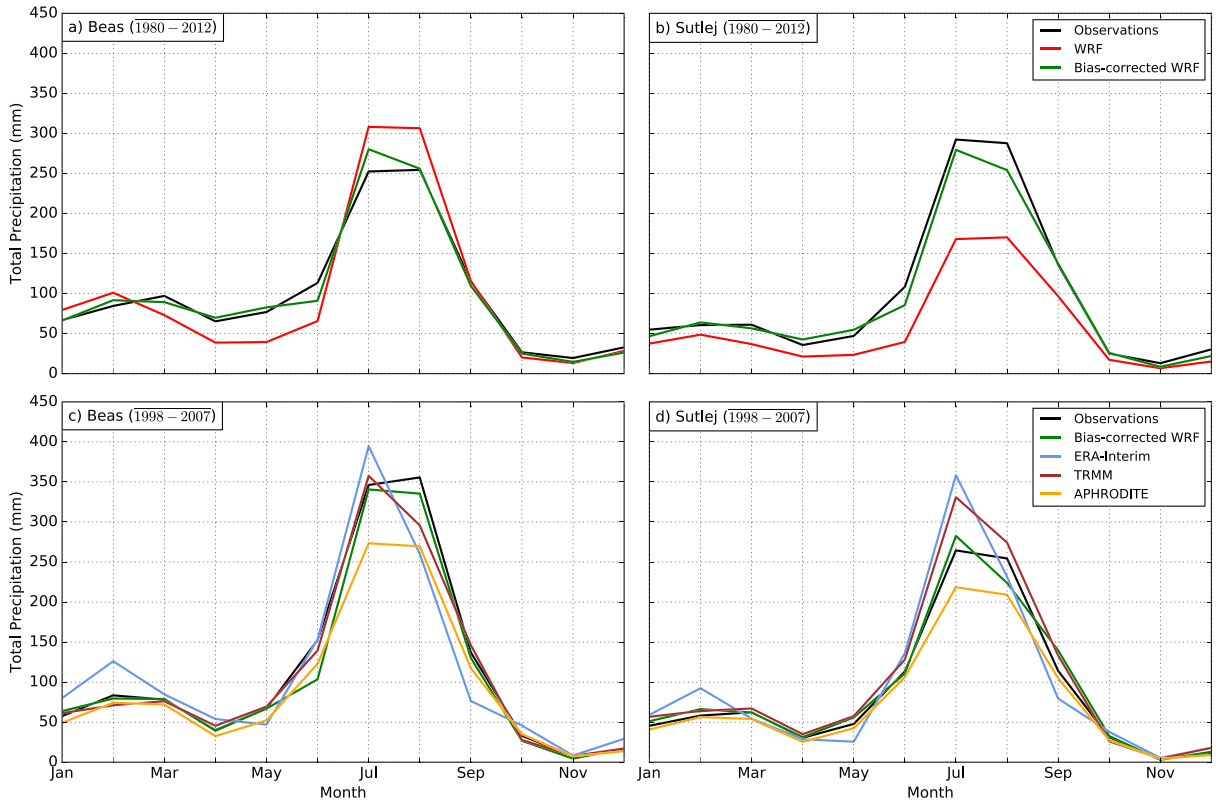

Figure 4. Comparison of (a) Beas and (b) Sutlej basin-averaged monthly precipitation from the in situ observations (black), Weather Research and Forecasting (WRF) output at a spatial resolution of 5 km (red), and bias-corrected WRF output (green) for the time period 1980 to 2012. (c and d) As (a) and (b) but comparing the in situ observations (black), bias-corrected WRF output (green), ERA-Interim (blue), TRMM (brown), and APHRODITE (yellow) for the time period 1998 to 2007.

during the monsoon, in combination with a dry bias during the premonsoon (Figure 4a). For both basins, the WRF output shows an excellent agreement with the observations when bias-corrected. Table 2 shows that by bias-correcting the WRF output, the mean precipitation bias for the Sutlej basin during the monsoon period has reduced from −87.5 to −17 mm, while the dry bias during the premonsoon period for the Beas basin has reduced from −32.1 to 5.1 mm.

Figure 5 presents a comparison of daily precipitation percentiles. For all seasons, the WRF model output is characterized by a systematic underestimation of low-intensity daily precipitation amounts of less than 10 mm per day, which is particularly apparent for the Sutlej basin during the premonsoon and monsoon. Although the representation of moderate to high daily precipitation amounts in the range of 10 to 100 mm per day is generally improved, the model also underestimates daily precipitation amounts in this range in the Sutlej basin during both the premonsoon and monsoon. Overall, the WRF model shows a greater skill in reproducing daily precipitation for the Beas basin compared to the Sutlej during the monsoon. The systematic underestimate in daily precipitation is largely removed by bias correcting the WRF output, although this does also result in an overestimation of low-intensity precipitation events for some seasons. Although the bias correction does not change the total number of wet/dry days in a year, applying an independent-sample *t* test showed that there was no statistically significant difference between the modeled and observed annual mean total number of wet days in either basin for the period 1980 to 2012.

In order to explore the cause of the dry bias in the Sutlej basin, Figure 6 shows the diurnal variation of WRF modeled precipitation for each basin and season. For both basins and all seasons with the exception of post-monsoon, there is an afternoon peak in precipitation. However, the model also shows an early morning precipitation peak at around 0600 LT in the Beas basin during the monsoon (Figure 6c), which is not apparent in the Sutlej basin. Note that as subdaily in situ observations are not available, it is not possible to say whether such peaks actually occur. However, additional analysis of the WRF output also showed a

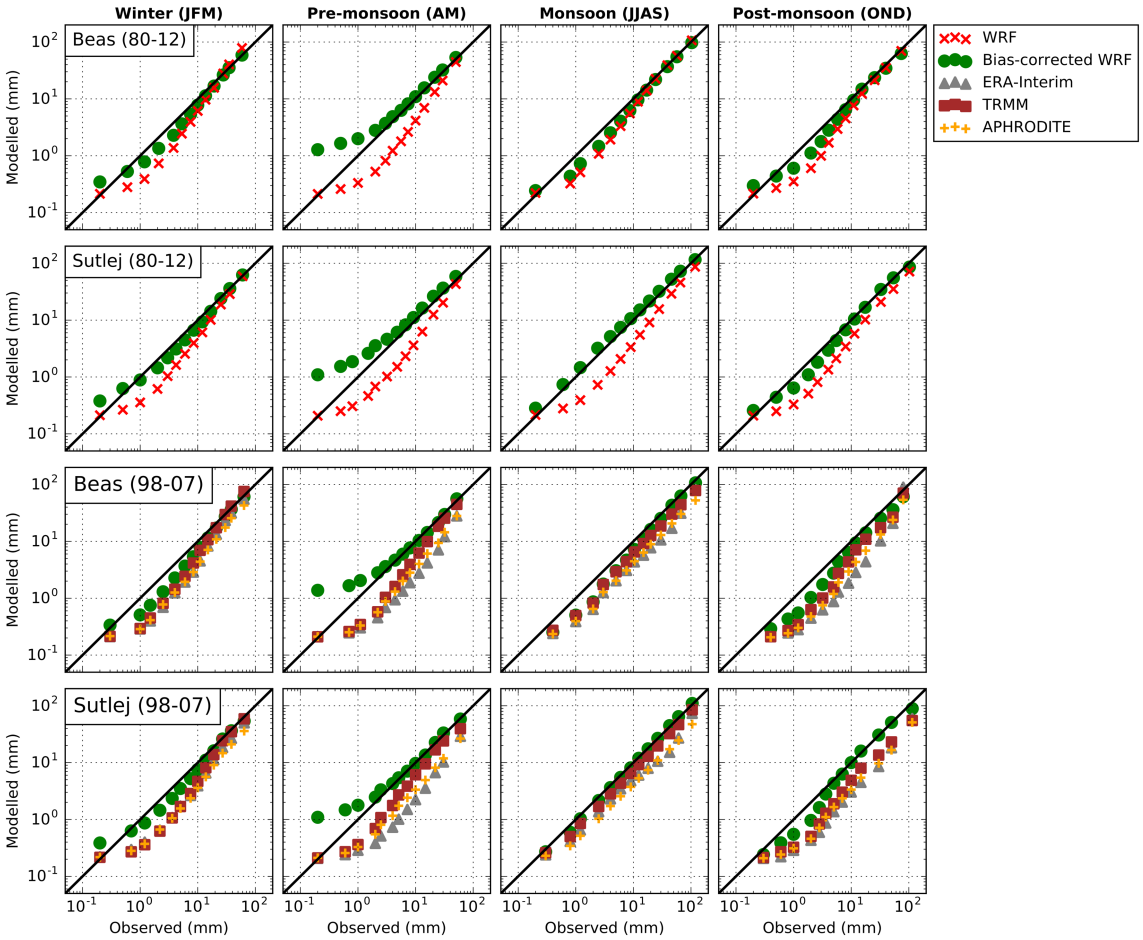

Figure 5. (top row) Comparison of seasonally and basin-averaged daily precipitation percentiles (1st, 5th, 10th 20th, 30th, 40th, 50th, 60th, 70th, 80th, 90th, 95th, and 99th) from the in situ observations and Weather Research and Forecasting (WRF) output at a spatial resolution of 5 km for the Beas basin for the time period 1980 to 2012. (second row) As top row but for the Sutlej basin. Seasons are defined as winter (January-February-March, far left column), premonsoon (April-May, column second to the left), monsoon (June-July-August-September, column second to the right), and postmonsoon (October-November-December, far right column). The lower two rows are analogous to the upper two rows, but comparing daily precipitation percentiles for bias-corrected WRF output, ERA-Interim, TRMM, and APHRODITE for the time period 1998 to 2007. Results are calculated for all nonzero precipitation days, defined as amounts ≥0.2mm per day.

bimodal cycle of precipitation in the adjacent Ravi and Yamuna river basins during the monsoon (not shown). This suggests that a failure to simulate this morning peak in precipitation is the explanation for the dry bias in the Sutlej basin during the monsoon. Enhanced precipitation in the morning would be expected in theory due to enhanced near-surface convergence of katabatic flow, resulting in upward

Table 2
Summary of the Basin-Averaged Error Statistics (Bias, Correlation Coefficient, and RMSE) for Annual and Seasonal Precipitation for the Beas and Sutlej Basins Based on Output From the WRF Model at a Spatial Resolution of 5 km and Bias-Corrected WRF Output (Shown in Brackets) for the Time Period 1980 to 2012

		Annual	Winter	Premonsoon	Monsoon	Postmonsoon
Beas	Bias (mm)	−15.3 (−2.4)	1.7 (−0.4)	−32.1 (5.1)	15.2 (0.3)	−5.7 (−4.3)
	Correlation coefficient	0.33* (0.48*)	0.75* (0.74*)	0.66* (0.53*)	0.76* (0.63*)	0.68* (0.76*)
	RMSE (mm)	275.4 (226.7)	41.2 (31.2)	47.6 (41.5)	106.5 (84.7)	26.7 (25.1)
Sutlej	Bias (mm)	−470.7 (−74.4)	−17.8 (−3.1)	−19.0 (7.3)	−87.5 (−17.0)	−9.7 (−4.0)
	Correlation coefficient	0.16 (0.41*)	0.80* (0.83*)	0.64* (0.59*)	0.60* (0.64*)	0.82* (0.89*)
	RMSE (mm)	547.4 (259.4)	30.0 (25.2)	31.3 (30.5)	135.0 (100.2)	22.8 (18.9)

Note. Asterisks indicate that the correlation coefficient is statistically significant at the 95% confidence level.
Abbreviation: RMSE: root-mean-square error; WRF: Weather Research and Forecasting.

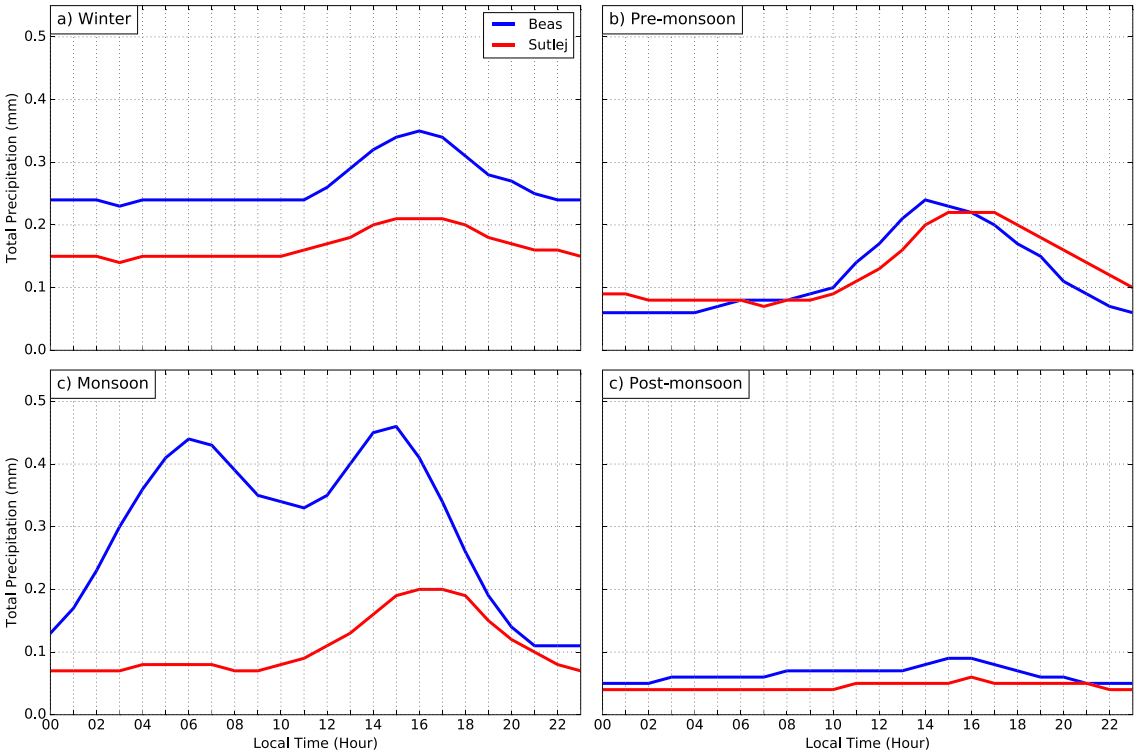

Figure 6. Seasonally and basin-averaged diurnal cycle of hourly precipitation based on output from the Weather Research and Forecasting (WRF) model at a spatial resolution of 5 km for the period 1980 to 2012 in the Beas (blue) and Sutlej (red) basins for (a) winter, (b) premonsoon, (c) monsoon, and (d) postmonsoon.

motion that can cause convection, as has been reported over other locations focused on south-facing slopes of the Himalaya [see, e.g., Bhatt & Nakamura, 2005; Orr et al., 2017; Prasad, 1974).

Further examination of the WRF output for the monsoon period (Figure 7) shows that moisture is initially transported over the lower elevation/western section of the Beas basin during the early morning, before it is subsequently deflected to the right (looking downwind) so that it passes over the lower elevation/western section of the Sutlej basin. Most of the moisture is transformed into precipitation over the Beas basin, resulting in considerably less moisture reaching the Sutlej and consequently much less precipitation. This suggests that the dry bias over the Sutlej basin could be partly due to excessive precipitation over the Beas. Figure 7 also shows analogous results for the afternoon period, which is characterized by a relatively uniform westerly transport of moisture from over the lower elevation regions of both basins, resulting in subsequent precipitation.

3.2. Assessment of Other Gridded Precipitation Datasets

In this section we assess how well ERA-Interim, TRMM, APHRODITE, and bias-corrected WRF output reproduce the in situ observations for the period 1998 to 2007 (for which they all overlap). Here, the selected ERA-Interim, TRMM, and APHRODITE data, and the bias-corrected WRF output, are based on the nearest-neighbor approach to the observations.

The error statistics shown in Table 3 for annual precipitation demonstrates that the performance of TRMM and bias-corrected WRF output are largely comparable for the Beas basin, and superior to APHRODITE; for example, they both have a wet bias of around 5 to 7 mm, and a RMSE of around 16 to 19 mm. However, although ERA-Interim has a smaller wet bias of 1.3 mm, it has a much larger RMSE of 39.2 mm and lower correlation coefficient of 0.94 (suggesting that its low overall bias is a result of cancelation of errors). By comparison, for annual precipitation in the Sutlej basin, the bias-corrected WRF output is superior to TRMM (as well as APHRODITE and ERA-Interim); for example, bias-corrected WRF output has a bias (RMSE) of 3.0 mm (13.2 mm) compared to 13.3 mm (21.9 mm) for TRMM. For monthly precipitation, Figures 4c and 4d demonstrate that the three gridded datasets agree better with the observations for the premonsoon,

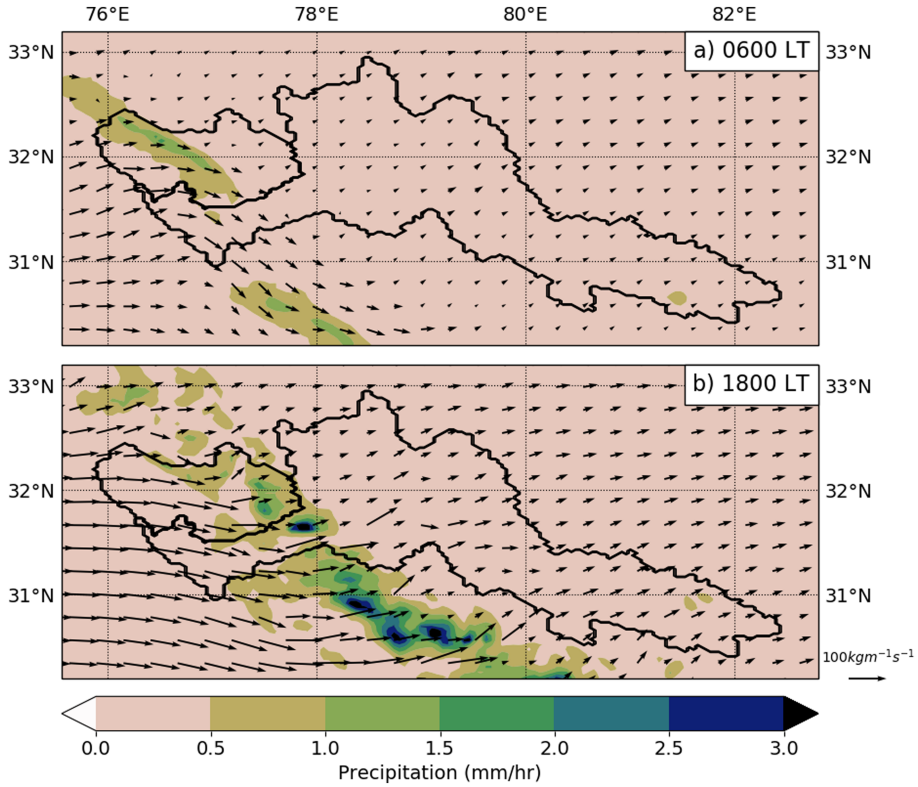

Figure 7. Mean column-integrated horizontal moisture flux (vectors, kg · m^{-1} · s^{-1}) and precipitation (shading, mm/hr) over the Beas and Sutlej basins at (a) 0600 LT and (b) 1500 LT, based on output from the Weather Research and Forecasting (WRF) model at a spatial resolution of 5 km during the monsoon season for the time period 1980 to 2012.

postmonsoon, and winter periods (and therefore largely with the bias-corrected WRF output) compared to the monsoon. For the monsoon, APHRODITE considerably underestimates the peak precipitation for both basins, while ERA-Interim tends to overestimate it. For the Beas basin, TRMM does a reasonable job of representing the peak in monsoon precipitation but overestimates it for the Sutlej basin. However, none of the gridded datasets perform as well as the bias-corrected WRF output for the monsoon period. Figure 4c also shows that ERA-Interim is characterized by periods of both wet and dry biases, explaining its low overall value for annual bias. Similarly, Figure 5 shows that TRMM, APHRODITE, and ERA-Interim all present a dry bias in both basins for low- and medium-intensity daily precipitation amounts for all seasons and that the bias-corrected WRF output agrees best with the observations (despite overestimating drizzle during the premonsoon season). Here, ERA-Interim is the least accurate, showing

Table 3
Summary of the Basin-Averaged Error Statistics (Bias, Correlation Coefficient, and RMSE) for Annual Precipitation for the Beas and Sutlej Basins Based on Bias-Corrected WRF Output at a Spatial Resolution of 5 km, ERA-Interim, TRMM, and APHRODITE for the Time Period 1998 to 2007

	Beas basin			Sutlej basin		
Dataset	Bias (mm)	RMSE (mm)	Correlation Coefficient	Bias (mm)	RMSE (mm)	Correlation Coefficient
Bias-corrected WRF	−7.4	15.8	0.99	3.0	13.2	0.99
ERA-Interim	−1.3	39.2	0.94	7.6	33.0	0.95
TRMM	−5.0	18.7	0.99	13.3	21.9	0.99
APHRODITE	−21.3	34.7	1.00	−11.4	19.3	1.00

Note. All correlation coefficients reported are statistically significant at the 95% confidence level. The WRF, ERA-Interim, TRMM, and APHRODITE results are derived from the nearest grid point to the *in situ* observations.
Abbreviations: APHRODITE: Asian Precipitation Highly Resolved Observational Data Integration Towards Evaluation of Water Resources; TRMM: Tropical Rainfall Measuring Mission; WRF: Weather Research and Forecasting.

Table 4
Mean and Standard Deviation (Shown in Brackets) of the Annual Number of Wet Days for the Beas and Sutlej Basins From In Situ Observations, Bias-Corrected WRF Output at a Spatial Resolution of 5 km, ERA-Interim, TRMM, and APHRODITE for the time period 1997 to 2008

Basin	Observations	Bias-corrected WRF	ERA-Interim	TRMM	APHRODITE
Beas	85 (9)	96 (11)	189* (11)	123* (11)	155* (8)
Sutlej	69 (6)	75 (8)	158* (5)	114* (10)	147* (6)

Note. Asterisks mark differences that are statistically significant at the 99% confidence level. Wet days are defined as daily accumulated precipitation ≥0.2 mm. Abbreviations: APHRODITE: Asian Precipitation Highly Resolved Observational Data Integration Towards Evaluation of Water Resources; TRMM: Tropical Rainfall Measuring Mission; WRF: Weather Research and Forecasting.

a strong dry bias for all precipitation intensities during all seasons. Note that the gridded datasets tend to agree better with the observations for high-intensity precipitation events.

Table 4 compares the mean annual number of wet days (defined as days receiving more than 0.2 mm of precipitation) estimated by the gridded datasets and the bias-corrected WRF model output with observations. The total number of wet days is overestimated by all three gridded datasets for both basins (despite Figure 5 showing that these datasets have a dry bias at daily timescales), especially by ERA-Interim and APHRODITE, which show respectively 77% and 67% more wet days than observed. An independent-sample *t* test showed that the differences between the datasets and observations are statistically significant (at the 99% confidence level). However, by far the best agreement with the observations is for the bias-corrected WRF output, which is not statistically different compared to observations.

Figure 8 focuses on the spatial pattern of annual precipitation over the entire Beas and Sutlej catchments, as well as the contribution made by each season to the annual total. Given the good performance of the bias-corrected WRF output (albeit based on comparison against stations located at relatively low altitudes [see Figure 1b], ranging in elevation from 284 to 3,639 m asl), we assume that it also gives the best insight into the precipitation characteristics over the high-altitude interior of the catchments, that is, that the relationship between elevation and the a and b parameters that are used to compute P^* throughout the Beas and Sutlej catchments (see section 2.3) also holds in these regions. On annual timescales, the bias-corrected WRF output shows a maximum in precipitation over the lower elevation regions located over the western side of the catchments, with the majority (~80%) falling during the monsoon (consistent with precipitation produced by orographic lifting of moist south-easterly winds associated with the monsoon). Section 2.3 showed that the elevation dependence was statistically robust during the period June to October (as well as other months), inferring higher confidence in the bias-corrected WRF output during the monsoon period. The bias-corrected WRF output also shows the dry region of the Zanda Valley in the upper reaches of the Sutlej basin, as well as a local peak in precipitation located around the source of the Sutlej (near lakes Manasarovar and Rakshastal) that occurs mainly during the monsoon. The bias-corrected WRF output also shows that negligible precipitation falls during the postmonsoon season and that whatever small amount of precipitation that falls during the premonsoon is concentrated within the high-altitude interior. Figure 8 also includes a column showing raw/uncorrected WRF output, which shows that the greatest differences are below around 3,000 m in both the Beas and the Sutlej basins; that is, the impact of the bias correction is to redistribute precipitation below this altitude (particularly by moving excess precipitation at higher elevations down to lower elevations), while largely preserving the raw values at elevations greater than 3,000 m. The most striking feature of the three gridded datasets is their similarity and the considerable differences compared to the bias-corrected WRF output. For example, all three gridded datasets clearly underestimate (overestimate) precipitation over the wet (dry) regions of the catchments, particularly during the monsoon, that is, underrepresenting the heterogeneity, which is attributable to factors such as grid spacing and the lack of in situ stations at high elevations.

3.3. Precipitation Extremes and Persistence

Figure 9 presents spatial patterns of the precipitation indices used in this study, expressed as annual means for the period 1998 to 2007. As with the patterns of precipitation (Figure 8), the indices based on ERA-Interim, TRMM, and APHRODITE data differ considerably from those based on bias-corrected WRF output. For precipitation extremes, the Rx5day index based on bias-corrected WRF output exhibits comparatively

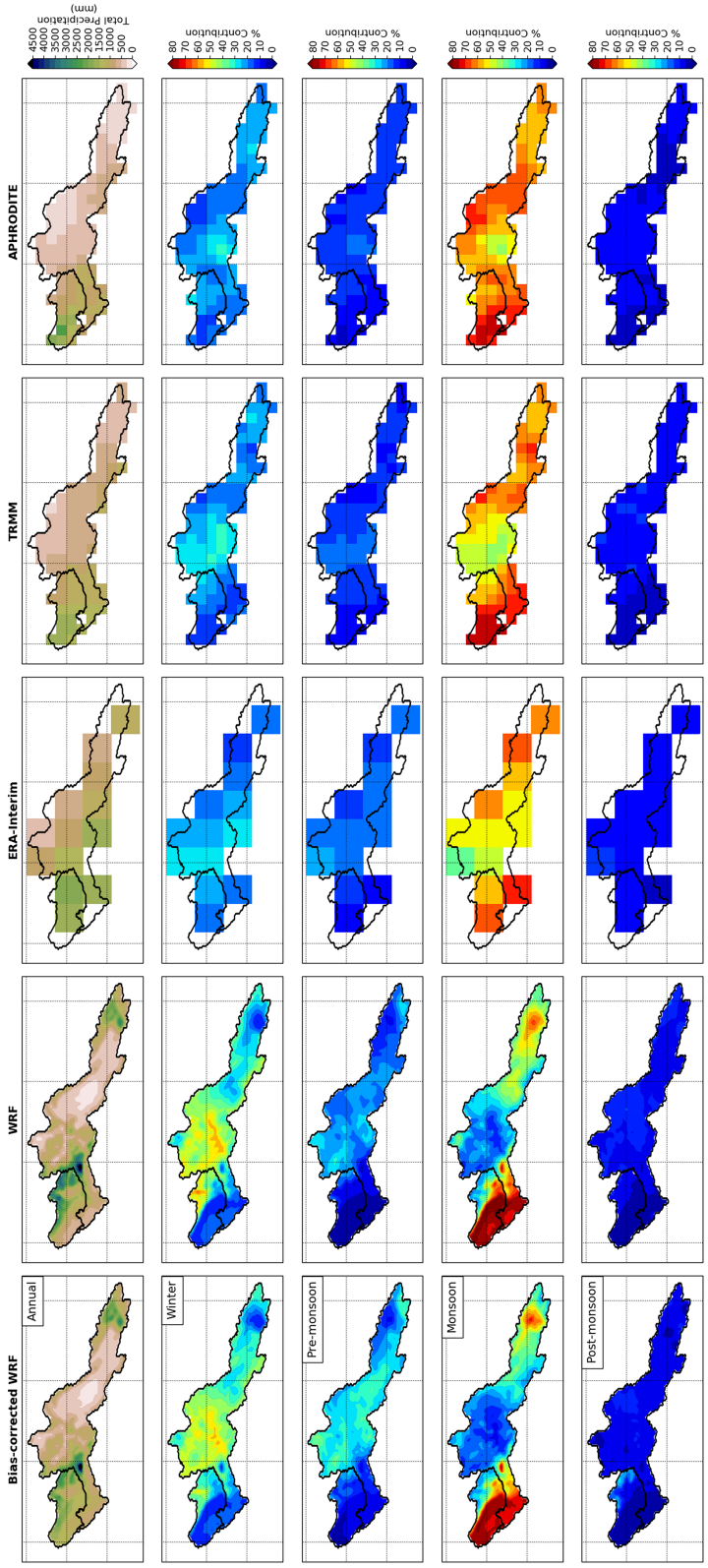

Figure 8. (top row) Comparison of the spatial distribution of annual precipitation (mm) over the Beas and Sutlej basins from bias-corrected Weather Research and Forecasting (WRF) output at a spatial resolution of 5 km, WRF output at a spatial resolution of 5 km, ERA-Interim, Tropical Rainfall Measuring Mission (TRMM), and Asian Precipitation Highly Resolved Observational Data Integration Towards Evaluation of Water Resources (APHRODITE) for the time period 1998 to 2007. (other rows) As top row but showing the subsequent contribution from winter, premonsoon, monsoon, and postmonsoon seasons to the annual total (%).

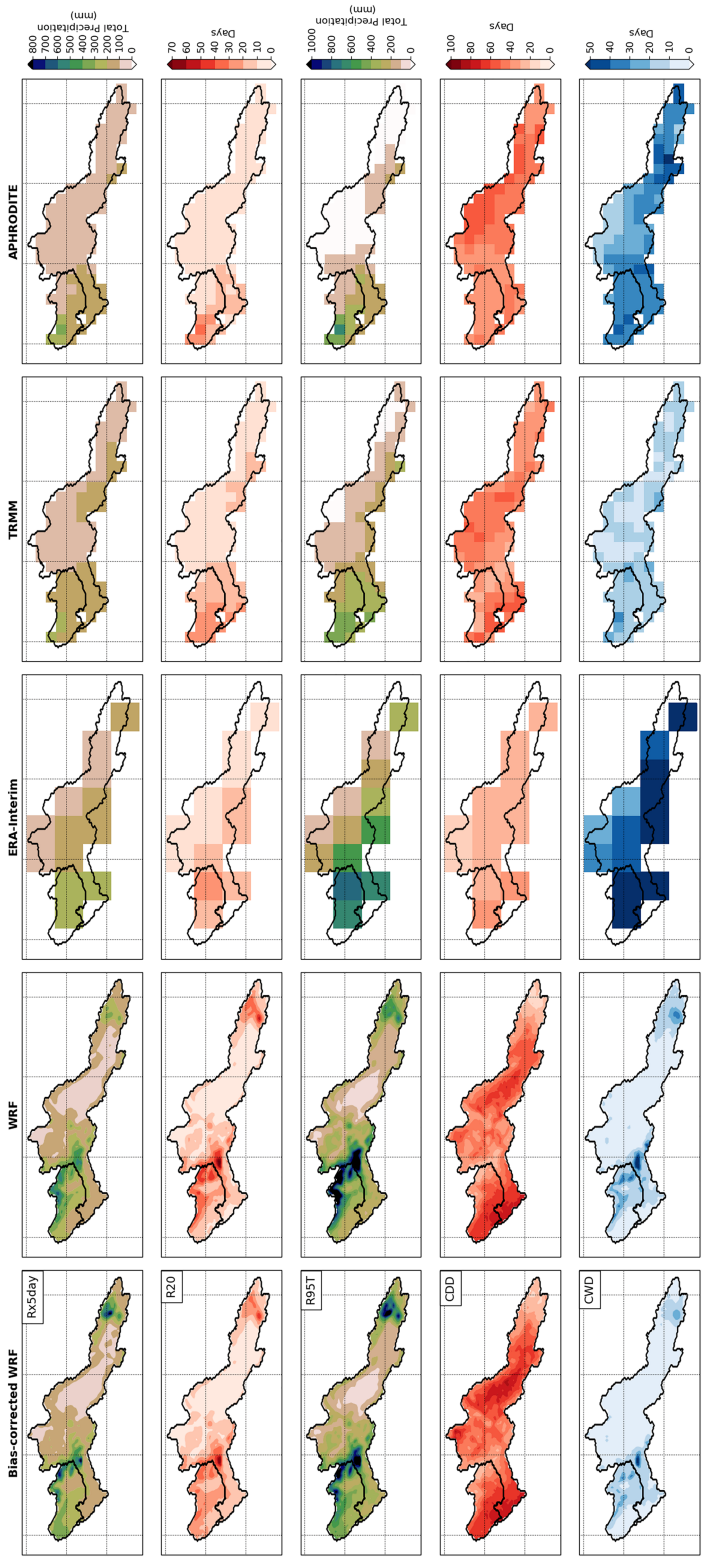

Figure 9. Comparison of the annually averaged spatial distribution of the Rx5day (mm), R20 (days), R95T (mm), consecutive dry day (CDD; days), and consecutive wet day (CWD; days) precipitation indices (aligned top to bottom) over the Beas and Sutlej basins from bias-corrected Weather Research and Forecasting (WRF) output at a spatial resolution of 5 km, WRF output at a spatial resolution of 5 km, ERA-Interim, Tropical Rainfall Measuring Mission (TRMM), and Asian Precipitation Highly Resolved Observational Data Integration Towards Evaluation of Water Resources ((APHRODITE; from left to right) for the time period 1998 to 2007. See section 2.4 for definition of the indices.

large values of around 800 mm over the western side of the catchments (in the narrow Sutlej river valley, near the Baspa-Sutlej confluence, located downstream of Kalpa and upstream of Sarhan) and near the source of the Sutlej on its eastern side, and minimum values of less than 100 mm over the Zanda Valley (see Figure 1 b for locations). This spatial pattern is broadly matched in the R20 index based on the bias-corrected WRF output, which shows that the wettest location is near the Baspa-Sutlej confluence with around 70 days per year exceeding a daily precipitation total of 20 mm. The three gridded datasets again fail to capture these localized maxima and minima, resulting in much smoother/broader fields. The R95T index based on the bias-corrected WRF output also shows a maximum of around 1,000 mm near the Baspa-Sutlej confluence of the Sutlej basin. High values of R95T index based on bias-corrected WRF output are also found in the northern part of the Beas basin and at the source of the Sutlej River. By comparison, R95T is particularly poorly captured by the gridded datasets, which is not surprising given the underrepresentation of daily high-intensity precipitation events (Figure 5). Figure 9 also includes values based on the raw/uncorrected WRF output, which although demonstrate broadly similar patterns of localized maxima and minima compared to the bias-corrected WRF output (like Figure 8) also show considerable differences in amplitude below around 3,000 m, while largely preserving the raw values at elevations greater than 3,000 m. For persistence, the CDD index based on bias-corrected WRF output indicates that the Zanda Valley and the western region are also the location of the maximum number of CDDs (reaching over 80 days), while dry periods are less persistent at the source of the Sutlej. The CWD index shows a maximum number of CWDs over the narrow Sutlej valley (around 50 days) and the source of the Sutlej, and a minimum in the Zanda Valley. All three gridded datasets overestimate (underestimate) the persistence of wet (dry) days across the two catchments. As expected, the patterns and amplitude of localized maxima and minima based on the raw WRF output and bias-corrected WRF output were broadly similar for both the indices representing persistence.

4. Discussion and Conclusions

The need to provide accurate estimates of precipitation over catchments in the HKKH for assessing its hydrology and water resource systems, as well as hydro-meteorological hazards, is widely recognized. While dynamically downscaled reanalysis or global climate model data (using regional climate models) are being increasingly used to provide precipitation estimates over specific regions in the HKKH (e.g., Akhtar et al., 2008; Ali et al., 2015; Li et al., 2016; Narula & Gosain, 2013; Nepal, 2016; ul-Hasson, 2016), their accuracy has yet to be conclusively proven as studies comparing model output and measurements, and the impact of bias correction on the model output, are still limited in both number and scope. Therefore, in this study, we focused on comprehensively assessing the ability of bias-correcting regional climate model to reproduce the observed detailed patterns of precipitation in the HKKH region by examining the performance of a high-resolution WRF model hindcast simulation generated for a long period of time, over a large region (encompassing two catchments, the Beas and the Sutlej), and assessed against a large number of in situ precipitation measurements. For the Sutlej basin, we find that the raw (uncorrected) model output exhibited a considerable dry bias in annual, monthly, and (particularly low-intensity) daily precipitation amounts. For the Beas basin, the simulation of precipitation was more accurate, although biases still existed. Applying the nonlinear bias-correction method (proposed by Leander & Buishand, 2007) to the model output resulted in much better estimates of precipitation (over both basins and at all temporal scales examined) in comparison to the available in situ observations. However, the largest impact of the bias-correction method was to redistribute precipitation below altitudes of around 3,000 m, while largely preserving the raw values at elevations greater than 3,000 m. A significant number of in situ observations could not be included in this study for a range of reasons, for example, failing standard quality control checks. While we believe that the remaining data set is the best available, further improvements in precipitation estimation could undoubtedly be achieved if higher quality station data with more spatiotemporal coverage were available, particularly above 3,000 m in the Sutlej basin.

We further showed that precipitation output from ERA-Interim reanalysis and two gridded precipitation datasets (TRMM and APHRODITE) that are available for this region are also characterized by considerable biases, which are broadly comparable in magnitude to those in the raw WRF model output. Moreover, the gridded datasets were markedly poorer at estimating the frequency of wet days compared to the model output. The poor performance of the gridded datasets over regions characterized by sharp gradients in precipitation (caused by the interaction between complex topographic features and regional scale atmospheric

circulation systems) is to be expected given that the spatial resolution of these datasets is larger than the spatial variability of precipitation. Consequently, it was shown that the bias-corrected WRF precipitation output was more accurate than the gridded datasets, suggesting that it is more suitable for use in impact studies for forcing hydrological and water system models and has further implications on the potential of regional climate modeling approaches to predict future changes in water resources in the HKKH region. Note that the basin-wide precipitation patterns estimated by the bias-corrected WRF output are broadly consistent with suggestions from Singh and Jain (2003) and Jain et al. (2010) that approximately 40–60% of the annual accumulation of these basins falls in the winter at high-elevations (in the form of frozen precipitation).

It is speculated that the cause of the dry bias over the Sutlej basin in the raw WRF model output is related to a failure to represent an early-morning maximum in precipitation during the monsoon period. Such a peak is apparent in the simulated output for the Beas basin and also reported over other locations focused on south facing slopes of the HKKH (e.g., Bhatt & Nakamura, 2005; Orr et al., 2017; Prasad, 1974). However, confirmation of its existence was hampered by the unavailability of subdaily station data. It was further speculated that this is related to excessive precipitation falling upstream (over the Beas), resulting in a moisture-deficit as the air passes over the Sutlej. It is also likely that the bias is related to the representation of localized diurnal mountain-valley winds, which play a key role in inducing convection. Adequate representation of these winds in regional climate models is a long-standing issue, with a number of previous studies highlighting the difficulty of representing them in the HKKH region (e.g., Bhatt & Nakamura, 2006; Norris et al., 2017; Orr et al., 2017; Sato, 2013; Shrestha & Deshar, 2014).

The bias-corrected WRF precipitation output is especially valuable to understand vulnerable regions, which are susceptible to precipitation extremes. By exploring various precipitation indices, we identified three broad regions within the Beas and Sutlej catchments that are particularly susceptible to such extremes: (1) the narrow Sutlej river valley (i.e., the Baspa-Sutlej confluence, which is the wettest region in the model), (2) the Manali and Dhauladhar mountain range (which is the wettest region in the Beas basin), and (3) the source of the Sutlej river (including Mount Kailash and lakes Manasarovar and Rakshastal, due to the occurrence of extreme daily precipitation amounts). The identification of these regions as being currently susceptible to precipitation extremes has implications for their future state, suggesting that they may be particularly vulnerable to continued increases in precipitation extremes under future climate scenarios. Projections based on outputs from coarse-resolution CMIP5 (Coupled Model Intercomparison Project phase 5) global climate model projections suggest that precipitation extremes are generally expected to intensify over the HKKH region in the future (Panday et al., 2014; Wu et al., 2017). However, our results also suggest that downscaling coarse-resolution climate model projections is critical to understand the regional detail of precipitation extremes over specific regions of the HKKH.

To conclude, we have demonstrated the benefits of bias-corrected high-resolution regional climate model output over two Himalayan catchments and shown that it provides better estimates of mean and extreme precipitation compared to reanalyses and gridded precipitation products. The modeling methodology employed here is equally applicable to similar river basins across the HKKH region, where it could be utilized to make much needed improvements to hydro-climatic services (Widmann et al., 2017). Further work will focus on using our high-resolution regional climate model to downscale outputs from CMIP5 model projections over the Beas and Sutlej basins to evaluate the impacts on precipitation of climate change from the middle to late 21st century, which will be used for subsequent hydrological impact studies (e.g., Lutz et al., 2014) as well as an improved understanding of precipitation extremes.

Acknowledgments
We are grateful for the comments from three reviewers, which helped to improve this paper. This research formed part of the joint UK-India "Sustaining water resources for food, energy & ecosystem services in India" program and was funded by the UK Natural Environment Research Council (grants NE/N015592/1, NE/N015541/1, and NE/N016394/1) and the Indian Ministry of Earth Sciences (grant number MES-1023-CED) under the Newton-Bhabha fund. The raw and bias-corrected precipitation output from the WRF hindcast can be accessed at the UK Polar Data Centre (Bannister et al., 2019). We would like to thank the Bhakra Beas Management Board and the Indian Meteorological Department for collecting the in situ precipitation measurements we used for the bias-correction and validation of the WRF model, as well as to Hendrik Wulf for passing them on to us. The authors of this paper do not have the legal right to make this dataset publicly available and suggest that any readers interested in obtaining it refer to Wulf et al. (2016). Finally, we wish to thank Hayley Bannister for writing the code for the bias correction of the model output.

References

Akhtar, M., Ahmad, N., & Booij, M. J. (2008). The impact of climate change on the water resources of Hindukush–Karakorum–Himalaya region under different glacier coverage scenarios. *Journal of Hydrology*, *355*(1-4), 148–163. https://doi.org/10.1016/j.hydrol.2008.03.015

Ali, S., Li, D., Congbin, F., & Khan, F. (2015). Twenty first century climatic and hydrological changes over the Upper Indus Basin of Himalayan region of Pakistan. *Environmental Research Letters*, *10*, 1–20. https://doi.org/10.1088/1748-9326/10/1/014007

Andermann, C., Bonnet, S., & Gloaguen, R. (2011). Evaluation of precipitation data sets along the Himalayan front. *Geochemistry, Geophysics, Geosystems*, *12*, Q07023. https://doi.org/10.1029/2011GC003513

Anders, A. M., Roe, G. H., Hallet, B., Montgomery, D. R., Finnegan, N. J., & Putkonen, J. (2006). Spatial patterns of precipitation and topography in the Himalaya. *Geological Society of America Special Papers*, *398*, 39–53. https://doi.org/10.1130/2006.2398(03)

Bannister, D., Orr, A., & Phillips, T. (2019). Model-simulated and bias-corrected daily total precipitation from a reanalysis-driven Weather Research and Forecasting simulation of the Beas and Sutlej river basins in the Himalaya, 1980 to 2012 (Version 1.0) [Data set], UK Polar

Data Centre, Natural Environment Research Council, UK Research & Innovation. https://doi.org/10.5285/74fab393-2718-4bdb-b229-190ae72a9fe1.

Bhardwaj, A., Ziegler, A. D., Wasson, R. J., & Chow, W. T. L. (2017). Accuracy of rainfall estimates at high altitude in the Garhwal Himalaya (India): A comparison of secondary precipitation products and station rainfall measurements. *Atmospheric Research*, *188*, 30–38. https://doi.org/10.1016/j.atmosres.2017.01.005

Bhatt, B. C., & Nakamura, K. (2005). Characteristics of monsoon rainfall around the Himalayas revealed by TRMM precipitation radar. *Monthly Weather Review*, *133*, 149–165. https://doi.org/10.1175/MWR-2846.1

Bhatt, B. C., & Nakamura, K. (2006). A climatological-dynamical analysis associated with precipitation around the southern part of the Himalayas. *Journal of Geophysical Research*, *111*, D02115. https://doi.org/10.1029/2005JD006197

Bonekamp, P. N. J., Collier, E., & Immerzeel, W. W. (2018). The impact of spatial resolution, land use, and spinup time on resolving spatial precipitation patterns in the Himalayas. *Journal of Hydrometeorology*, *19*, 1565–1581. https://doi.org/10.1175/JHM-D-17-0212.s1

Bookhagen, B., & Burbank, D. W. (2010). Toward a complete Himalayan hydrological budget: Spatiotemporal distribution of snowmelt and rainfall and their impact on river discharge. *Journal of Geophysical Research*, *115*, F03019. https://doi.org/10.1029/2009JF001426

Bordoy, R., & Burlando, P. (2013). Bias correction of regional climate model simulations in a region of complex orography. *Journal of Applied Meteorology and Climatology*, *52*, 82–101. https://doi.org/10.1175/JAMC-D-11-0149.1

Burbank, D. W., Bookhagen, B., Gabet, E. J., & Putkonen, J. (2012). Modern climate and erosion in the Himalaya. *Comptes Rendus Geoscience*, *344*, 610–626. https://doi.org/10.1016/j.crte.2012.10.010

Chen, F., & Dudhia, J. (2001). Coupling an advanced land surface-hydrology model with the Penn State-NCAR MM5 modeling system. Part I: Model implementation and sensitivity. *Monthly Weather Review*, *129*, 569–585. https://doi.org/10.1175/1520-0493(2001)129<0569:CAALSH>2.0.CO;2

Chinnasamy, P., Bharati, L., Bhattarai, U., Khadka, A., Dahal, V., & Wahid, S. (2015). Impact of planned water resource development on current and future water demand in the Koshi River basin, *Nepal*. *Water International*, *40*, 1004–1020. https://doi.org/10.1080/02508060.2015.1099192

Collier, E., & Immerzeel, W. W. (2015). High-resolution modeling of atmospheric dynamics in the Nepalese Himalaya. *Journal of Geophysical Research*, *120*, 9882–9896. https://doi.org/10.1002/2015JD02326

Das, S., Ashrit, R., & Moncrieff, M. W. (2006). Simulation of a Himalayan cloudburst event. *Journal of Earth System Science*, *115*, 299–313. https://doi.org/10.1007/BF02702044

Dee, D. P., Uppala, S. M., Simmons, A. J., Berrisford, P., Poli, P., Kobayashi, S., et al. (2011). The ERA-Interim reanalysis: Configuration and performance of the data assimilation system. *Quarterly Journal of the Royal Meteorological Society*, *137*, 553–597. https://doi.org/10.1002/qj.828

Dimri, A. P., Chevuturi, A., Niyogi, D., Thayyen, R. J., Ray, K., Tripathi, S. N., et al. (2017). Cloudbursts in Indian Himalayas: A review. *Earth-Science Reviews*, *168*, 1–23. https://doi.org/10.1016/j.earscirev.2017.03.006

Dudhia, J. (1989). Numerical study of convection observed during the winter monsoon experiment using a mesoscale two-dimensional model. *Journal of the Atmospheric Sciences*, *46*, 3077–3107. https://doi.org/10.1175/1520-0469(1989)046<3077:NSOCOD>2.0.CO;2

Eriksson, M., Xu, J., Shrestha, A. B., Vaidya, R. A., Nepal, S., & Sandström, K. (2009). *The changing Himalayas: Impact of climate change on water resources and livelihoods in the greater Himalayas* (p. 24). Kathmandu, Nepal: International Centre for Integrated Mountain Development.

Friedl, M., & Sulla-Menashe, D. (2015). MCD12Q1 MODIS/Terra+Aqua Land Cover Type Yearly L3 Global 500 m SIN Grid V006 [Data set], NASA EOSDIS Land Processes DAAC. https://doi.org/10.5067/MODIS/MCD12Q1.006

Garnier, B. J., & Ohmura, A. (1968). A method of calculating the direct shortwave radiation income of slopes. *Journal of Applied Meteorology*, *7*, 796–800. https://doi.org/10.1175/1520-0450(1968)007<0796:AMOCTD>2.0.CO;2

Ghosh, S., & Dutta, S. (2012). Impact of climate change on flood characteristics in Brahmaputra basin using a macro-scale distributed hydrological model. *Journal of Earth System Science*, *121*(3), 637–657. https://doi.org/10.1007/s12040-012-0181-y

Hall, D. K., Riggs, G. A., Salomonson, V. V., DiGirolamo, N. E., & Bayr, K. J. (2002). MODIS snow-cover products. *Remote Sensing of Environment*, *83*, 181–194. https://doi.org/10.1016/S0034-4257(02)00095-0

Huffman, G. J., Adler, R. F., Bolvin, D. T., Gu, G., Nelkin, E. J., Bowman, K. P., et al. (2007). The TRMM multisatellite precipitation analysis (TMPA): Quasi-global, multiyear, combined-sensor precipitation estimates at fine scales. *Journal of Hydrometeorology*, *8*, 38–55. https://doi.org/10.1175/JHM560.1

Hussain, S., Song, X., Ren, G., Hussain, I., Han, D., & Zaman, M. H. (2017). Evaluation of gridded precipitation data in Hindu Kush-Karakoram-Himalaya mountainous area. *Hydrological Sciences Journal*, *62*, 2393–2405. https://doi.org/10.1080/02626667.2017.1384548

Immerzeel, W. W., Wanders, N., Lutz, A. F., Shea, J. M., & Bierkens, M. F. P. (2015). Reconciling high-altitude precipitation in the upper Indus basin with glacier mass balances and runoff. *Hydrology and Earth System Sciences*, *19*, 4673–4687. https://doi.org/10.5194/hess-19-4673-2015

Jain, S. K., Goswami, A., & Saraf, A. K. (2010). Snowmelt runoff modelling in a Himalayan basin with the aid of satellite data. *International Journal of Remote Sensing*, *31*, 6603–6618. https://doi.org/10.1080/01431160903433893

Jarvis, A., H. I. Reuter, Nelson,A., & Guevara, E. (2008). Hole-filled SRTM for the globe Version 4, available from the CGIAR-CSI SRTM 90 m Database. http://srtm.csi.cgiar.org

Kain, J. S. (2004). The Kain–Fritsch convective parameterization: An update. *Journal of Applied Meteorology*, *43*, 170–181. https://doi.org/10.1175/1520-0450(2004)043<0170:TKCPAU>2.0.CO;2

Karki, R., ul Hasson, S., Schickhoff, U., Scholten, T., & Böhner, J. (2017). Rising precipitation extremes across Nepal. *Climate*, *5*. https://doi.org/10.3390/cli5010004

Lafon, T., Dadson, S., Buys, G., & Prudhomme, C. (2013). Bias correction of daily precipitation simulated by a regional climate model: A comparison of methods. *International Journal of Climatology*, *33*, 1367–1381. https://doi.org/10.1002/joc.3518

Leander, R., & Buishand, T. A. (2007). Resampling of regional climate model output for the simulation of extreme river flows. *Journal of Hydrology*, *332*, 487–496. https://doi.org/10.1016/j.jhydrol.2006.08.006

Li, H., Xu, C.-Y., Beldring, S., Merete Tallaksen, L., & Jain, S. K. (2016). Water resources under climate change in Himalayan basins. *Water Resources Management*, *30*, 843–859. https://doi.org/10.1007/s11269-015-1194-5

Li, L., Gochis, D. J., Sobolowski, S., & Mesquita, M. D. (2017). Evaluating the present annual water budget of a Himalayan headwater river basin using a high-resolution atmosphere-hydrology model. *Journal of Geophysical Research: Atmospheres*, *122*, 4786–4807. https://doi.org/10.1002/2016JD026279

Lutz, A. F., Immerzeel, W. W., Shrestha, A. B., & Bierkens, M. F. P. (2014). Consistent increase in High Asia's runoff due to increasing glacier melt and precipitation. *Nature Climate Change*, *4*, 587–592. https://doi.org/10.1038/nclimate2237

Ma, L., Zhang, T., Frauenfeld, O. W., Ye, B., Yang, D., & Qin, D. (2009). Evaluation of precipitation from the ERA-40, NCEP-1, and NCEP-2 reanalyses and CMAP-1, CMAP-2, and GPCP-2 with ground-based measurements in China. *Journal of Geophysical Research*, *114*, D09105. https://doi.org/10.1029/2008JD011178

Maussion, F., Scherer, D., Finkelnburg, R., Richters, J., Yang, W., & Yao, T. (2011). WRF simulation of a precipitation event over the Tibetan Plateau, China—An assessment using remote sensing and ground observations. *Hydrology and Earth System Sciences*, *15*, 1795–1817. https://doi.org/10.5194/hessd-7-3551-2010

Medina, S., Houze, R. A., Kumar, A., & Niyogi, D. (2010). Summer monsoon convection in the Himalayan region: Terrain and land cover effects. *Quarterly Journal of the Royal Meteorological Society*, *136*, 593–616. https://doi.org/10.1002/qj.601

Meng, J., Li, L., Hao, Z., Wang, J., & Shao, Q. (2014). Suitability of TRMM satellite rainfall in driving a distributed hydrological model in the source region of Yellow River. *Journal of Hydrology*, *509*, 320–332. https://doi.org/10.1016/j.hydrol.2013.11.049

Mlawer, E. J., Taubman, S. J., Brown, P. D., Iacono, M. J., & Clough, S. A. (1997). Radiative transfer for inhomogeneous atmospheres: RRTM, a validated correlated-k model for the longwave. *Journal of Geophysical Research*, *102*, 16663–16682. https://doi.org/10.1029/97JD00237

Momblanch, A., Papadimitriou, L., Jain, S. K., Kulkarni, A., Ojha, C. S. P., Adeloye, A. J., & Holman, I. P. (2019). Untangling the water-food-energy-environment nexus for global change adaptation in a complex Himalayan water resource system. *Science of the Total Environment*, *655*, 35–47. https://doi.org/10.1016/j.scitotenv.2018.11.045

Morrison, H., Thompson, G., & Tatarskii, V. (2009). Impact of cloud microphysics on the development of trailing stratiform precipitation in a simulated squall line: Comparison of one-and two-moment schemes. *Monthly Weather Review*, *137*, 991–1007. https://doi.org/10.1175/2008MWR2556.1

Nakanishi, M., & Niino, H. (2006). An improved Mellor–Yamada level-3 model: Its numerical stability and application to a regional prediction of advection fog. *Boundary-Layer Meteorology*, *119*, 397–407. https://doi.org/10.1007/s10546-005-9030-8

Narula, K. K., & Gosain, A. K. (2013). Modelling hydrology, groundwater recharge and non-point nitrate loadings in the Himalayan Upper Yamuna basin. *Science of the Total Environment*, *468*. https://doi.org/10.1016/j.scitotenv.2013.01.022

Nepal, S. (2016). Impacts of climate change on the hydrological regime of the Koshi river basin in the Himalayan region. *Journal of Hydro-environment Research*, *10*, 76–89. https://doi.org/10.1016/j.her.2015.12.001

Norris, J., Carvalho, L. M. V., Jones, C., Cannon, F., Bookhagen, B., Palazzi, E., & Tahir, A. A. (2017). The spatiotemporal variability of precipitation over the Himalaya: Evaluation of one-year WRF model simulation. *Climate Dynamics*, *49*(5-6), 2179–2204. https://doi.org/10.1007/s00382-016-3414-y

Norris, J., Carvalho, L. M. V., Jones, C., Cannon, F., & F. (2015). WRF simulations of two extreme snowfall events associated with contrasting extratropical cyclones over the western and central Himalaya. *Journal of Geophysical Research: Atmospheres*, *120*, 3114–3138. https://doi.org/10.1002/2014JD022592

Orr, A., Listowski, C., Couttet, M., Collier, E., Immerzeel, W. W., Deb, P., & Bannister, D. (2017). Sensitivity of simulated summer monsoonal precipitation in Langtang Valley, Himalaya to cloud microphysics schemes in WRF. *Journal of Geophysical Research: Atmospheres*, *122*, 6298–6318. https://doi.org/10.1002/2016JD025801

Palazzi, E., von Hardenberg, J., & Provenzale, A. (2013). Precipitation in the Hindu-Kush Karakoram Himalaya: Observations and future scenarios. *Journal of Geophysical Research: Atmospheres*, *118*, 85–100. https://doi.org/10.1029/2012JD018697

Panday, P. K., Thibeault, J., & Frey, K. E. (2014). Changing temperature and precipitation extremes in the Hindu Kush-Himalayan region: An analysis of CMIP3 and CMIP5 simulations and projections. *International Journal of Climatology*, *35*, 3058–3077. https://doi.org/10.1002/joc.4192

Pfeffer, W. T., Arendt, A. A., Bliss, A., Bolch, T., Cogley, J. G., Gardner, A. S., et al., & The Randolph Consortium (2014). The Randolph Glacier Inventory: A globally complete inventory of glaciers. *Journal of Glaciology*, *60*, 537–552. https://doi.org/10.3189/2014JoG13J176

Potter, E. R., Orr, A., Willis, I. C., Bannister, D., & Salerno, F. (2018). Dynamical drivers of the local wind regime in a Himalayan valley. *Journal of Geophysical Research: Atmospheres*, *123*, 13,186–13,202. https://doi.org/10.1029/2018JD029427

Prasad, B. (1974). Diurnal variation of rainfall in Brahmaputra valley. *Mausam*, *25*, 245–250.

Remesan, R., & Holman, I. P. (2015). Effect of baseline meteorological data selection on hydrological modelling of climate change scenarios. *Journal of Hydrology*, *528*, 631–642. https://doi.org/10.1016/j.hydrol.2015.06.026

Roy, S. S. (2008). A spatial analysis of extreme hourly precipitation patterns in India. *International Journal of Climatology*, *29*, 345–355. https://doi.org/10.1002/joc.1763

Sanjay, J., Krishnan, R., Shrestha, A. B., Rajbhandari, R., & Ren, G.-Y. (2017). Downscaled climate change projections for the Hindu Kush Himalaya region using CORDEX South Asia regional climate models. *Advances in Climate Change Research*, *8*, 185–198. https://doi.org/10.1016/j.accre.2017.08.003

Sato, T. (2013). Mechanism of orographic precipitation around the Meghalaya Plateau associated with intraseasonal oscillation and the diurnal cycle. *Monthly Weather Review*, *141*, 2451–2466. https://doi.org/10.1175/MWR-D-12-00321.1

Sharma, B. R., & De Condappa, D. (2013). Opportunities for harnessing the increased contribution of glacier and snowmelt flows in the Ganges basin. *Water Policy*, *15*, 9–25. https://doi.org/10.2166/wp.2013.008

Shrestha, D., & Deshar, R. (2014). Spatial Variations in the diurnal pattern of precipitation over Nepal Himalayas. *Nepal Journal of Science and Technology*, *15*, 57–64. https://doi.org/10.3126/njst.v15i2.12116

Shrestha, M., Acharya, S. C., & Shrestha, P. K. (2017). Bias correction of climate models for hydrological modelling—Are simple methods still useful? *Meteorological Applications*, *24*, 531–539. https://doi.org/10.1002/met.1655

Shukla, S., Kansal, M. L., & Jain, S. K. (2016). Snow cover area variability assessment in the upper part of the Satluj river basin in India. *Geocarto International*, *32*, 1285–1306. https://doi.org/10.1080/10106049.2016.1206975

Sigdel, M., & Ma, Y. (2017). Variability and trends in daily precipitation extremes on the northern and southern slopes of the central Himalaya. *Theoretical and Applied Climatology*, *130*(1-2), 571–581. https://doi.org/10.1007/s00704-016-1916-5

Singh, P., & Jain, S. K. (2003). Modelling of streamflow and its components for a large Himalayan basin with predominant snowmelt yields. *Hydrological Sciences Journal*, *48*, 257–276. https://doi.org/10.1623/hysj.48.2.257.44693

Skamarock, W. C., Klemp, J. B., Dudhia, J., Gill, D. O., Barker, D. M., Duda, M. G., et al. (2008). A Description of the Advanced Research WRF Version 3. NCAR Technical Note, NCAR/TN-475+STR, National Center for Atmospheric Research. Boulder, CO. https://doi.org/10.5065/D68S4MVH

Terink, W., Hurkmans, R. T. W. L., Torfs, P. J. J. F., & Uijlenhoet, R. (2010). Evaluation of a bias correction method applied to downscaled precipitation and temperature reanalysis data for the Rhine basin. *Hydrology and Earth System Sciences*, *14*, 687–703. https://doi.org/10.5194/hess-14-687-201

Teutschbein, C., & Seibert, J. (2012). Bias correction of regional climate model simulations for hydrological climate-change impact studies: Review and evaluation of different methods. *Journal of Hydrology*, *456-457*, 12–29. https://doi.org/10.1016/j.jhydrol.2012.05.052

ul-Hasson, S. (2016). Future water availability from Hindukush-Karakoram-Himalaya upper Indus Basin under conflicting climate changes scenarios. *Climate*, *4*(3), 40. https://doi.org/10.3390/cli4030040

Widmann, M., R. Blake, K. P. Sooraj, A. Orr, J. Sanjay, A. Karumuri Mitra, et al. (2017). Current opportunities and challenges in developing hydro-climatic services in the Himalayas, Indian UK Water Centre (IUKWC) report.

Winiger, M., Gumpert, M., & Yamout, H. (2005). Karakorum-Hindukush-western Himalaya: assessing high-altitude water resources. *Hydrological Processes*, *19*, 2329–2338. https://doi.org/10.1002/hyp.5887

Wu, J., Xu, Y., & Gao, X.-J. (2017). Projected changes in mean and extreme climates over Hindu Kush Himalayan region by 21 CMIP5 models. *Advances in Climate Change Research*, *8*, 176–184. https://doi.org/10.1016/j.accre.2017.03.001

Wulf, H., Bookhagen, B., & Scherler, D. (2010). Seasonal precipitation gradients and their impact on fluvial sediment flux in the Northwest Himalaya. *Geomorphology*, *118*, 13–21. https://doi.org/10.1016/j.geomorph.2009.12.003

Wulf, H., Bookhagen, B., & Scherler, D. (2016). Differentiating between rain, snow, and glacier contributions to river discharge in the western Himalaya using remote-sensing data and distributed hydrological modeling. *Advances in Water Resources*, *88*, 152–169. https://doi.org/10.1016/j.advwatres.2015.12.004

Yadav, R. K., Kumar, K. R., & Rajeevan, M. (2012). Characteristic features of winter precipitation and its variability over northwest India. *Journal of Earth System Science*, *121*, 611–623. https://doi.org/10.1007/s12040-012-0184-8

Yatagai, A., Kamiguchi, K., Arakawa, O., Hamada, A., Yasutomi, N., & Kitoh, A. (2012). APHRODITE: Constructing a long-term daily gridded precipitation dataset for Asia based on a dense network of rain gauges. *Bulletin of the American Meteorological Society*, *93*, 1401–1415. https://doi.org/10.1175/BAMS-D-11-00122.1

Yin, Z.-Y., Zhang, X., Liu, X., Colella, M., & Chen, X. (2008). An assessment of the biases of satellite rainfall estimates over the Tibetan Plateau and correction methods based on topographic analysis. *Journal of Hydrometeorology*, *9*, 301–326. https://doi.org/10.1175/2007JHM903.1